Available online at www.sciencedirect.com
ScienceDirect
Journal of Organometallic Chemistry 692 (2007) 1–9
Journal of Organometallic Chemistry
www.elsevier.com/locate/jorganchem

$[MoFe_3S_4]^{3+}$ and $[MoFe_3S_4]^{2+}$ cubane clusters containing a pentamethylcyclopentadienyl molybdenum moiety

Takashi Komuro [a], Hiroyuki Kawaguchi [b], Jianping Lang [a], Takayuki Nagasawa [a], Kazuyuki Tatsumi [a,*]

[a] *Research Center for Materials Science, and Department of Chemistry, Graduate School of Science, Nagoya University, Furo-cho, Chikusa-ku, Nagoya 464-8602, Japan*
[b] *Coordination Chemistry Laboratories, Institute for Molecular Science, Myodaiji, Okazaki 444-8595, Japan*

Received 27 April 2006; accepted 3 July 2006
Available online 5 September 2006

Abstract

A series of organometallic molybdenum/iron/sulfur clusters of the general formula $[Cp^*MoFe_3S_4L_n]^m$ ($Cp^* = \eta^5$-C_5Me_5; L = S^{t}Bu, SPh, Cl, I, $n = 3$, $m = 1-$; $L_n = I_2(P^tBu_3)$, $m = 0$; L = 2,6-diisopropylphenylisocyanide (ArNC), $n = 7$, $m = 1+$) have been synthesized. A cubane cluster $(PPh_4)[Cp^*MoFe_3S_4(S^tBu)_3]$ (**2**) was isolated from a self-assembly reaction of $Cp^*Mo(S^tBu)_3$ (**1**), $FeCl_3$, LiS^{t}Bu, and S_8 followed by cation exchange with PPh_4Br in CH_3CN, while an analogous cluster $(PPh_4)[Cp^*MoFe_3S_4(SPh)_3]$ (**3**) was obtained from the $Cp^*MoCl_4/FeCl_3/LiSPh/PPh_4Br$ reaction system or from a ligand substitution reaction of **2** with PhSH. Treatment of **2** with benzoyl chloride gave rise to $(PPh_4)[Cp^*MoFe_3S_4Cl_3]$ (**4**), which was in turn converted to $(PPh_4)[Cp^*MoFe_3S_4I_3]$ (**5**) by the reaction with NaI. A neutral cubane cluster $Cp^*MoFe_3S_4I_2(P^tBu_3)$ (**6**) was generated upon treating **5** with P^tBu_3. Although reduction of **4** by cobaltocene under the presence of ArNC resulted in a disproportionation of the cubane core to give $Fe_4S_4(ArNC)_9Cl$ (**7**), a similar reduction reaction of **5** produced $[Cp^*MoFe_3S_4(ArNC)_7]I$ (**8**), where the $MoFe_3S_4$ core was retained. The crystal structures of **4**–**6**, and **8** were determined by the X-ray analysis.

Keywords: Molybdenum; Iron: sulfide; Cubane cluster; Cyclopentadienyl

1. Introduction

It has been well documented that transition metal sulfide clusters play key roles in biological systems [1a] and in industrial processes as catalysts such as dehydrosulfurization [1b]. Development of rational synthetic routes to transition metal sulfide clusters continues to be a major subject in inorganic chemistry [2], and in particular the synthesis of molybdenum/iron/sulfide clusters have attracted attention in relation to the cluster active sites of nitrogenase [3].

Tetrathiamolybdate, tetrathiatungstate, and related mononuclear sulfide/thiolate complexes have been used as building blocks for the synthesis of Mo(W)-based sulfide clusters [4], and di- and tri-nuclear metal sulfides have also been reacted with late transition metal complexes in order to obtain heterometallic sulfide clusters of high nuclearity [5,6]. For instance, we have developed convenient routes to heterometallic sulfide clusters based on organometallic tris-sulfide complexes of molybdenum and tungsten, $(PPh_4)[Cp^*MS_3]$ (M = Mo, W) [7]. Cubane clusters of transition metal sulfides can also be assembled into large clusters. For example, it was reported that the reaction of $[(Cl_4cat)(CH_3CN)MoFe_3S_4Cl_3]^{2-}$ with $NaBPh_4$ in the presence of PEt_3 gave an edge-linked double cubane cluster $Mo_2Fe_6S_8(PEt_3)_6(Cl_4cat)_2$ [8]. We also reported the synthesis of $[Mo_2Fe_2S_4]^{4+}$ cubane cluster, $Cp^*{}_2Mo_2Fe_2S_4Cl_2$, from $Cp^*Mo(S^tBu)_3$ (**1**) and $FeCl_3$, and its reaction with

* Corresponding author. Tel.: +81 52 789 2943.
E-mail address: i45100a@nucc.cc.nagoya-u.ac.jp (K. Tatsumi).

0022-328X/$ - see front matter © 2006 Elsevier B.V. All rights reserved.
doi:10.1016/j.jorganchem.2006.07.047

Li_2S_2 leading to aggregation of the cubane cluster into a cyclic tri-cubane cluster $[Cp^*_2Mo_2Fe_2S_4]_3(\mu\text{-}S_4)_3$ [9].

To expand the scope of Fe/Mo/S cluster syntheses, we examined a self-assembly reaction of $Cp^*Mo(S^tBu)_3$ (**1**) with $FeCl_3$ in the presence of LiS^tBu and elemental sulfur (S_8). This paper reports that the reaction, followed by a cation exchange with PPh_4Br, gave rise to a $MoFe_3S_4$ cubane cluster, $(PPh_4)[Cp^*MoFe_3S_4(S^tBu)_3]$ (**2**), and that the subsequent ligand exchange reactions generated a series of cubane clusters having a common Cp^*Mo fragment, $(PPh_4)[Cp^*MoFe_3S_4X_3]$ (X = SPh (**3**), Cl (**4**), I (**5**)). The reactions of **5** with P^tBu_3 and ArNC/cobaltocene to give $Cp^*MoFe_3S_4I_2(P^tBu_3)$ (**6**) and $[Cp^*MoFe_3S_4(ArNC)_7]I$ (**7**, ArNC = 2,6-diisopropylphenylisocyanide) are also reported.

2. Experimental

2.1. General procedures, materials, and solvents

All manipulations were carried out under an atmosphere of argon using a Schlenk technique, and solvents were dried by standard methods. $Cp^*Mo(S^tBu)_3$ (**1**) [7b], 2,6-diisopropylphenylisocyanide [10], and cobaltocene [11] was synthesized according to literature procedures, while P^tBu_3 was purchased from Kanto Kagaku and used as received. LiSPh and LiS^tBu were prepared from the reactions of PhSH and ^{t}BuSH with n-C_4H_9Li (1.6 M hexane solution) in THF at 0 °C prior to use. For the measurement of UV–Vis spectra, a U-best-30 spectrometer was used. Infrared spectra were recorded on a Parkin Elmer 2000FT-IR spectrometer. Elemental analyses were performed on a LECO-CHNS microanalyzer where the crystalline samples were sealed in thin silver tubes. Electrochemical studies were preformed with an ALS model-700 electrochemical analyzer, where the cell was equipped with a glassy carbon disk as working electrode, a Pt auxiliary electrode, and an SCE reference electrode. (^{n}Bu$_4$N)PF_6 was used as a supporting electrolyte.

2.2. Synthesis of $(PPh_4)[Cp^*MoFe_3S_4(S^tBu)_3]$ (2)

A THF (20 mL) solution of **1** (1.41 g, 2.83 mmol) was added to a mixture of $FeCl_3$ (1.37 g, 8.45 mmol) and LiS^tBu (25.4 mmol) in the same solvent (80 mL), and the subsequent addition of elemental sulfur (0.36 g, 11.2 mmol) produced a deep brown solution. After 4 h of stirring at room temperature, the solution was evaporated under vacuum to dryness. The resulting solid was dissolved in warm CH_3CN (60 mL) and the solution was filtered. A CH_3CN (30 mL) solution of PPh_4Br (0.95 g, 2.27 mmol) was added to the filtrate, and concentration of the solution gave a brown solid. Recrystallization from CH_3CN afforded 1.86 g of **2** (58%). ESI MS: *m/z* 796 ($[Cp^*MoFe_3S_4(S^tBu)_3]^-$). UV–Vis ($\lambda_{max}$, nm, ($\varepsilon_{max}$, $mol^{-1}\,dm^3\,cm^{-1}$) CH_3CN): 391(7700). Anal. Calc. for $C_{46}H_{62}Fe_3MoPS_7C_2H_3N$: C, 49.07 ; H, 5.58; N, 1.19; S, 19.10. Found: C, 49.44; H, 5.50; N, 1.30; S, 18.96%.

2.3. Synthesis of $(PPh_4)[Cp^*MoFe_3S_4(SPh)_3]$ (3)

Method A. Addition of a THF (60 mL) solution of LiSPh (47 mmol) into a slurry of Cp^*MoCl_4 (0.87 g, 2.3 mmol) in THF (15 mL) at 0 °C gave a dark red solution. The solution was stirred at room temperature for 1 h, to which a slurry of $FeCl_3$ (0.89 g, 7.0 mmol) and elemental sulfur (0.30 g, 9.35 mmol) in THF (40 mL) was added, to find that the color immediately turned deep brown. After the mixture was stirred for additional 6 h, volatile materials were removed in vacuo. The residue was dissolved in CH_3CN (20 mL) and centrifuged to remove an insoluble material. A solution of PPh_4Br (0.98 g, 2.3 mmol) in CH_3CN (20 mL) was added to the supernatant. Concentration of the supernatant and the subsequent cooling to −20 °C gave a brown powder, which was recrystallized from CH_3CN to yield brown needles of **3** (1.37 g, 48%). ESI MS: *m/z* 856 ($[Cp^*MoFe_3S_4(SPh)_3]^-$). UV–Vis (λ_{max}, nm, CH_3CN): 450 sh. Anal. Calc. for $C_{52}H_{50}Fe_3MoPS_7C_2H_3N$: C, 52.52; H, 4.33; N, 1.13; S, 18.18. Found: C, 52.31; H, 4.22; N, 1.14; S, 18.91%.

Method B. Benzenethiol (0.25 mL, 2.4 mmol) was added to a solution of **2** (0.87 g, 0.74 mmol) in CH_3CN (20 mL). The reaction mixture was stirred for 30 min, and the solution was concentrated slowly for 10 min to remove ^{t}BuSH. Addition of ether to the resulting solution and cooling to −20 °C gave rise to the deposition of **3** as black crystals in 72% (0.66 g).

2.4. Synthesis of $(PPh_4)[Cp^*MoFe_3S_4Cl_3]$ (4)

To a solution of **2** (2.13 g, 1.81 mmol) in CH_3CN (80 mL) was added 2.2 mL of benzoyl chloride (19 mmol). A color of the solution changed from dark yellow to brown. After 1 h of stirring at room temperature, the solution was concentrated. Slow addition of ether resulted in the precipitation of black crystals. The solution was decanted, and the crystals were washed with ether to give 1.16 g of **4** in 68% yield. ^{1}H NMR (CD_3CN): δ 7.6–8.0 (PPh_4), −4.74 (Cp^*, br). IR (KBr): 1588 (w), 1485 (m), 1441 (s), 1434 (s), 1119 (s), 1028 (w), 1003 (w), 755 (w), 728 (s), 692 (s), 409 (w) cm^{-1}. ESI MS: *m/z* 634 ($[Cp^*MoFeS_4Cl_3]^-$). UV–Vis (λ_{max}, nm): 340. Anal. Calc. for $C_{34}H_{35}Fe_3Cl_3MoPS_4$: C, 41.98; H, 3.63; S, 13.19. Found: C, 41.64; H, 3.56; S, 13.10%.

2.5. Synthesis of $(PPh_4)[Cp^*MoFeS_4I_3]$ (5)

Sodium iodide (0.43 g, 2.9 mmol) was added to **4** (0.40 g, 0.41 mmol) in CH_3CN (50 mL). The color of reaction mixture immediately became yellow-brown. The solution was stirred overnight at room temperature and was centrifuged to remove a white solid. Concentration of the solvent in vacuo resulted in the deposition of **5** as black microcrystals (0.40 g, 77%). ^{1}H NMR ($CDCl_3$): δ 7.6–8.5 (PPh_4), −4.16 (Cp^*, br). IR (KBr): 1483 (m), 1435 (s), 1376 (m), 1108 (s), 1024 (w), 997 (w), 749 (w), 723 (s),

689 (s), 526 (s), 409 (w) cm^{-1}. UV–Vis (λ_{max}, nm): 340. Anal. Calc. for $C_{34}H_{35}Fe_3I_3MoPS_4C_2H_3N$: C, 33.57; H, 2.97; N, 1.09; S, 9.96. Found: C, 33.58; H, 3.14; N, 0.98; S, 9.86%.

2.6. Synthesis of $Cp^*MoFe_3S_4I_2(P^tBu_3)$ (6)

P^tBu_3 (0.41 g, 2.0 mmol) in THF (45 mL) was added to a solution of **5** (1.43 g, 1.15 mmol) in CH_3CN (45 mL) at room temperature with stirring. After 4 h, the mixture was centrifuged and the solvent was removed in vacuo. The residue was washed with CH_3CN, CH_3OH, and ether, leaving crude **6** as black powder. Recrystallization from THF/hexane yielded black crystals of **6** (0.80 g, 71%). ^1H NMR ($CDCl_3$): δ 10.52 (P^tBu_3, br), −2.16 (Cp^*, br). IR (KBr): 2998 (s), 2953 (s), 2908 (s), 1481 (s), 1471 (s), 1443 (s), 1425 (s), 1393 (s), 1377 (s), 1172 (s), 1023 (s) cm^{-1}. UV–Vis (λ_{max}, nm (ε, $M^{-1}\,cm^{-1}$), THF): 340 (sh, 14000). Anal. Calc. for $C_{22}H_{42}Fe_3I_2MoPS_4$: C, 26.88; H, 4.31; S, 13.05. Found: C, 27.11; H, 4.33; S, 13.13%.

2.7. Reaction of $(PPh_4)[Cp^*MoFe_3S_4Cl_3]$ (4) with ArNC and Cp_2Co

Addition of a CH_3CN solution of cobaltocene (64 mg, 34 mmol) into a mixture of **4** (0.33 g, 0.34 mmol) and ArNC (0.40 g, 2.1 mmol) in 40 mL of CH_3CN caused an immediate precipitation of a brown powder. After 5 h of stirring at room temperature, the solution was decanted to leave crude $Fe_4S_4(ArNC)_9Cl$ (**7**) as brown powder. Recrystallization from toluene/hexane afforded black rods of **7** (0.12 g). IR (KBr): 2100 (s, ν_{NC}), 2060 (s, ν_{NC}) cm^{-1}. Anal. Calc. for $C_{117}H_{153}ClFe_4N_9S_4C_4H_8O$: C, 67.76; H,7.57; N, 5.88; S, 5.98. Found: C, 67.28; H, 7.70; N, 5.61; S, 6.20%.

2.8. Synthesis of $[Cp^*MoFe_3S_4(ArNC)_7]I$ (8)

A solution of cobaltocene (48 mg, 2.4 mmol) in 5 mL of CH_3CN was added to a stirred yellow-brown solution of **5** (0.31 g, 0.25 mmol) and ArNC (0.45 g, 2.4 mmol) in CH_3CN (40 mL) at room temperature. The solution turned dark brown. After the reaction mixture was stirred overnight, the solvent was removed in vacuo to leave a dark brown oil. The resulting oil was treated with toluene (100 mL) and centrifuged to remove an insoluble material. Concentration of the supernatant resulted in the deposition of **8** as dark brown crystals (0.45 g, 91%). IR (KBr): 2080 (s, ν_{NC}) cm^{-1}. UV–Vis (λ, nm): 340 (sh). Anal. Calc. for $C_{101}H_{134}Fe_3I_2MoN_7S_4C_7H_8$: C, 63.06; H, 6.96; N, 4.77; S, 6.24. Found: C, 63.21; H, 7.08; N, 4.28; S, 5.95%.

2.9. X-ray crystal structure determination

Crystal data, data collection, and refinement parameters for all structurally characterized complexes are summarized in Table 1. Single crystals of **4** and **5** were obtained from CH_3CN solutions. Slow diffusion of hexane into the

Table 1
Crystal data for $(PPh_4)[Cp^*MoFe_3S_4Cl_3]$ (**4**), $(PPh_4)[Cp^*MoFe_3S_4I_3]$ (**5**), $Cp^*MoFe_3S_4I_2(P^tBu_3)$ (**6**), and $[Cp^*MoFe_3S_4(ArNC)_7]I$ (**8**)

	4	5	6	8
Formula	$C_{34}H_{36}S_4Cl_3PFe_3Mo$	$C_{34}H_{36}S_4I_3PFe_3MoC_2H_3N$	$C_{22}H_{42}S_4I_2PFe_3Mo$	$C_{101}H_{134}N_7S_4IFe_3Mo2C_7H_8$
Molecular weight ($g\,mol^{-1}$)	972.70	1289.12	983.08	2149.12
Crystal system	Monoclinic	Monoclinic	Orthorhombic	Monoclinic
Space group	$P2_1/c$ (No. 14)	$P2_1/c$ (No. 14)	$Pbca$ (No. 61)	$P2_1/n$ (No. 14)
Color of crystal	Black	Black	Black	Black
Crystal size	$0.80\times0.20\times0.10$	$0.70\times0.30\times0.15$	$0.30\times0.25\times0.20$	$0.25\times0.10\times0.05$
a (Å)	18.100(5)	15.732(2)	18.7132(2)	16.7985(8)
b (Å)	11.677(9)	9.1851(4)	17.1809(2)	27.8763(3)
c (Å)	19.292(5)	30.7374(7)	21.2565(4)	24.5502(3)
β (°)	108.55(2)	92.936(1)		103.1322(4)
V (Å^3)	3862(3)	4435.8(4)	6834.2(3)	11195.7(4)
Z	4	4	8	4
ρ_{calc} ($g\,cm^{-3}$)	1.673	1.930	1.911	1.275
μ(Mo Kα) (cm^{-1})	19.09	35.75	37.15	8.89
Number of unique reflections	7159	8975	7721	24903
Number of observations data[a]	3511	7266	6615	11858
Number of parameters residuals	410	442	298	1145
R[b]	0.041	0.057	0.028	0.079
Rw[c]	0.046	0.072	0.040	0.079
GOF [d]	1.41	2.37	1.59	2.05

[a] Observation criterion $I > 3\sigma(I)$.
[b] $R = \sum\|F_o| - |F_c\|/\sum|F_o|$.
[c] $Rw = [\{\sum w(|F_o| - |F_c|)^2\}/\sum wF_o^2]^{1/2}$.
[d] $GOF = [\{\sum w(|F_o| - |F_c|)^2\}/(N_o - N_p)]^{1/2}$, where N_o and N_p denote the number of data and parameters.

THF solution gave crystals of **6**, while crystals of **8** were obtained from the toluene solution. Crystals of **4** suitable for X-ray analysis were mounted in glass capillaries and sealed under argon. Diffraction data were collected at room temperature on a Rigaku AFC7R diffractometer employing graphite-monochromated Mo Kα radiation ($\lambda = 0.710\,690$ Å) and using the ω–2θ scan technique. Refined cell dimensions and their standard deviations were obtained by least-squares refinements of 25 randomly selected centered reflections. Three standard reflections, monitored periodically for crystal decomposition or movement, showed slight intensity variation over the course of the data collections. The raw intensities were corrected for Lorentz and polarization effects. Empirical absorption corrections based on ψ scans were applied.

Crystals of **5**, **6**, and **8** were mounted at the top of a quartz fiber using grease, which were set on a Rigaku AFC7 equipped with a MSC/ADSC Quantum1 CCD detector. The measurements were made by using Mo Kα radiation at −100 °C under a cold nitrogen stream. Four preliminary data frames were measured at 0.5° increments of ω, in order to assess the crystal quality and calculate preliminary unit cell parameters. The intensity images were measured at 0.5 ° intervals of ω for duration of 87 s for **5**, 82 s for **6**, and 100 s for **8**. The frame data were integrated using a d*TREK program package, and the data sets were corrected empirically for absorption using the REQAB program.

All calculations were performed with a TEXSAN program package. All structures were solved by direct methods, and the structures were refined by full-matrix least squares. Anisotropic refinement was applied to all non-hydrogen atoms, and all the hydrogen atoms were put at calculated positions. Crystals of **5** and **8** contain crystal solvents, acetonitrile (**5**) and toluene (**8**), and the toluene carbon atoms of **8** were refined isotropically. Additional information is available as supporting information.

3. Results and discussion

3.1. Synthesis of $(PPh_4)[Cp^*MoFe_3S_4X_3]$ ($X = S^tBu$ (**2**), SPh (**3**), Cl (**4**), I (**5**))

We previously reported that the reaction of $Cp^*Mo(S^tBu)_3$(**1**) with $FeCl_3$ in THF resulted in C–S bond cleavage of the thiolate, yielding a $Mo_2Fe_2S_4$ cubane cluster $Cp^*_2Mo_2Fe_2S_4Cl_2$ [9]. Activation of the C–S bond was facilitated by an oxidant $FeCl_3$, suggesting that **1** may serve as a building block for another class of heteronuclear clusters if a suitable oxidant is employed. It is known that elemental sulfur (S_8) is capable of acting as an oxidizing reagent toward thiolato complexes [1a,12,13], and treatment of iron thiolato complexes with elemental sulfur was reported to generate various Fe/S/SR clusters such as $[Fe_2S_2(SR)_4]^{2-}$, $[Fe_3S_4(SR)_4]^{3-}$, and $[Fe_4S_4(SR)_4]^{2-}$ [12]. We also found that elemental sulfur promotes oxidation of the Mo(IV) center of **1**, producing an Mo(VI) complex $Cp^*Mo(S)_2(S^tBu)$ [9].

In this context, we examined the reaction of **1** with $FeCl_3$ in the presence of LiS^tBu and elemental sulfur, anticipating that this might provide a new synthetic route to molybdenum/iron/sulfide clusters. Thus, a THF solution of **1** was added to a mixture of $FeCl_3$ and LiS^tBu in the same solvent, and the subsequent addition of elemental sulfur gave a deep brown solution, from which a $MoFe_3S_4$ cubane cluster anion $[Cp^*MoFe_3S_4(S^tBu)_3]^-$ was generated. This cubane cluster was isolated as dark brown crystals of $(PPh_4)[Cp^*MoFe_3S_4(S^tBu)_3]$ (**2**), after the cation exchange reaction with PPh_4Br in CH_3CN. The yield of **2** reached 58%, when the molar ratio of the reactants was adjusted to **1**:$FeCl_3$:LiS^tBu:S:PPh_4Br = 1:3:9:1:0.8. Although assignment of oxidation numbers to the metal atoms in clusters is often obscure, one possible choice would be Mo(V) + 3Fe(II).

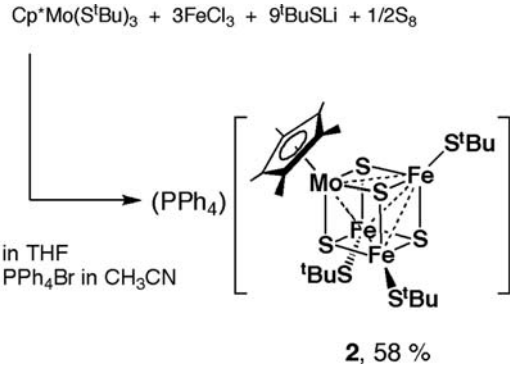

(1)

2, 58 %

Substitution reactions of the thiolate in **2** with anionic ligands were investigated. First, benzenethiol was found to react readily with complex **2** and to replace the *tert*-butylthiolate ligands, generating $(PPh_4)[Cp^*MoFe_3S_4(SPh)_3]$ (**3**) in 72% yield. This cluster anion was also assembled at room temperature from the reaction between Cp^*MoCl_4 and excess LiSPh in THF, which presumably generates $Cp^*Mo(SPh)_3$, and the subsequent addition of $FeCl_3$ (3 equiv) and elemental sulfur (4 equiv based on S). The phosphonium salt (**3**) was isolated in 48% yield, after a cation exchange with PPh_4Br in CH_3CN. As was mentioned earlier in this section, the $Mo_2Fe_2S_4$ cluster, $Cp^*_2Mo_2Fe_2S_4Cl_2$, was formed when **1** was treated with $FeCl_3$, where sulfide was presumably derived from *tert*-butylthiolate of **1** via C–S bond cleavage. In contrast, addition of elemental sulfur and lithium salt of *tert*-butylthiolate (or benzenethiolate) to the reaction system ended up with the $MoFe_3S_4$ clusters (**2** and **3**). It is likely that at least a part of the sulfide of **2** is originated from elemental sulfur, and a part could come from *tert*-butylthiolate via C–S bond rupture. In fact, decrease of elemental sulfur in the reaction of **1**/$FeCl_3$/LiS^tBu/S_8/PPh_4Br lowered the yield of **2**. In the case of the reaction of Cp^*MoCl_4/LiSPh/$FeCl_3$ in the absence of elemental sulfur, the $MoFe_3S_4$ cluster (**3**) could not be isolated, probably because C–S bond cleavage of benzenethiolate is more difficult compared with that of *tert*-butylthiolate

Method A

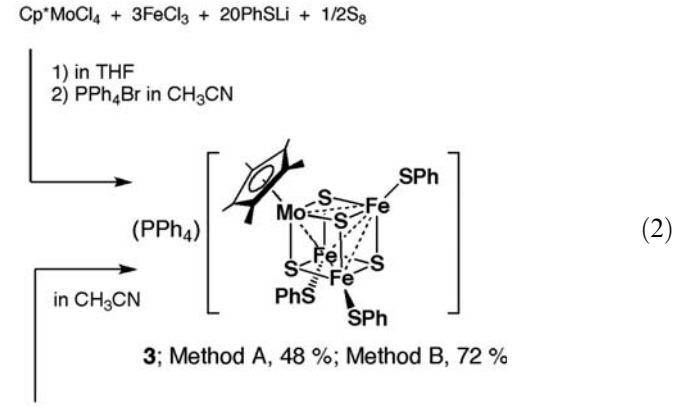

(2)

$(PPh_4)[Cp^*MoFe_3S_4(S^tBu)_3]$ + 3PhSH

2

Method B

It was also possible to substitute the thiolato ligand of **2** with chloride, then with iodide. Addition of an excess of benzoyl chloride to a CH_3CN solution of **2** resulted in the formation of $(PPh_4)[Cp^*MoFe_3S_4Cl_3]$ (**4**), which was obtained as black crystals in 68% yield. Further treatment of **4** with sodium iodide in CH_3CN gave rise to the iodide analogue of **4**, $(PPh_4)[Cp^*MoFe_3S_4I_3]$ (**5**). These synthetic methods to substitute thiolates on transition metal ions with halides are known, and have been used in the preparation of Fe/Mo/S and Fe/S clusters with chloride or iodide on Fe [14]. Conversely, treatment of **4** with 3 equiv of LiS^{t}Bu or LiSPh in CH_3CN regenerated corresponding thiolato derivatives **2** or **3** in good yields. During these ligand-substitution reactions, the common $MoFe_3S_4$ cubane core was retained. However, the iodide derivative **5** is less robust than **4**, and we have not been successful to prepare **2** and **3** by the analogous reactions **5** with thiolates

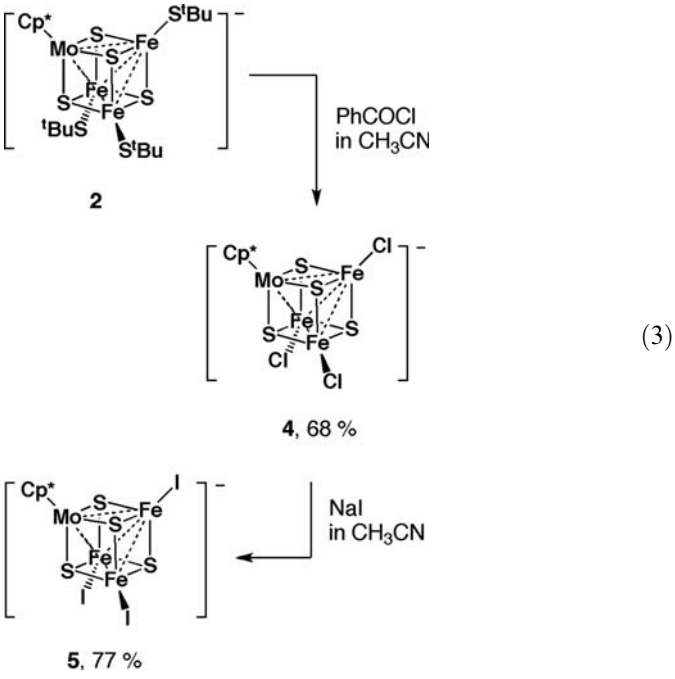

(3)

Combustion analyses of C, H, N, S for the crystalline samples of **2**–**5** are all in good agreement with the formulation, where **2** and **3** appear to be crystallized with CH_3CN as a crystal solvent. X-ray fluorescence microanalysis gave the reasonable Mo:Fe:S:P ratio expected for **2** and **3**, and Mo:Fe:S:P:Cl(I) ratios for **4** and **5**, respectively. Formation of the $MoFe_3S_4$ cluster anions in solution was also confirmed by the negative ESI mass spectra of **2**–**5**, which show the signals fitting in well with the calculated isotope patterns. The ^{1}H NMR spectra were measured for **4** and **5** in CD_3CN. The paramagnetic nature of these clusters is evident in the spectra, exhibiting broad Cp* signals at $\delta = -4.74$ and -4.16 for **4** and **5**, respectively. The cyclic voltammogram of **2**, **4** and **5** were measured in CH_3CN. Two quasi-reversible redox couples were observed for **2** and **4** in the region of reduction, while for **5** there appeared one quasi-reversible couple and one irreversible peak. The $E_{1/2}$ and E_p values are listed in Table 2. It is apparent that the $[MoFe_3S_4]^{3+}$ cubane core is more readily reduced as the ligand on Fe is substituted from S^{t}Bu to Cl and then to I. The quasi-reversible redox couples are comparable to those found for $[MoFe_3S_4Cl_3\{3,6\text{-}(C_3H_5)_2C_6H_2O_2\}(THF)]$, $[(C_2O_4)XMoFe_3S_4Cl_3]^{3-}$ (X = Cl, CN), and $[(mida)MoFe_3S_4Cl_3]^{2-}$, which range from -0.75 V to -1.13 V [14b,15].

The crystal structures of **4** and **5** were determined by X-ray diffraction analysis, and the selected metric parameters are summarized in Table 3. Because their structures are nearly identical, only the ORTEP drawing of the anion of **4** is presented in Fig. 1. The cubane core can be viewed as a distorted $MoFe_3$ tetrahedron, to which four sulfur atoms cap the trigonal faces. The average Mo–Fe and Fe–Fe distances of **4** (2.759 Å and 2.752 Å) and **5** (2.736 Å and 2.722 Å) are similar to those of $[(C_2O_4)XMoFe_3S_4Cl_3]^{3-}$ (X = Cl, CN; Mo–Fe, 2.747 Å; Fe–Fe, 2.718 Å) and $[(mida)MoFe_3S_4Cl_3]^{2-}$ (Mo–Fe, 2.730 Å; Fe–Fe, 2.737 Å) [15]. The observed short Mo–Fe and Fe–Fe distances indicate the presence of metal–metal bonding, and interestingly the average Mo–Fe bond distances are not very different from the average Fe–Fe distances despite the larger ionic radii of Mo. On the other hand, the Mo–S bond lengths are 0.04–0.05 Å longer than the Fe–S lengths. The other geometrical parameters are normal.

Table 2
Cyclic voltammetric data for **2**, **4**–**6**, and **8**[a]

Compound	Solvent	Reduction(V)[b]	Oxidation(V)[b]
2	CH_3CN	−1.27, qr; −1.44, qr	−0.10, irr, −0.40, qr
4	CH_3CN	−0.84, qr; −1.16, qr	0.04, irr
5	CH_3CN	−0.64, qr; −1.12, irr	
6	THF	−0.48, qr; −0.83, qr	0.15, irr
8	THF	−1.12, qr	−0.02, irr; 0.82, irr

[a] qr = Quasi-reversible redox couple, irr = irreversible signal.
[b] V vs. SCE; $E_{1/2}$ values for qr and E_p values for irr.

Table 3
Selected bond distances (Å) and angles (°) for $(PPh_4)[Cp^*MoFe_3S_4Cl_3]$ (**4**) and $(PPh_4)[Cp^*MoFe_3S_4I_3]$ (**5**)

	4	5
Mo–Fe1	2.752(2)	2.734(1)
Mo–Fe2	2.759(1)	2.734(1)
Mo–Fe3	2.767(1)	2.740(1)
Fe1–Fe2	2.727(2)	2.695(1)
Fe1–Fe3	2.768(2)	2.735(2)
Fe2–Fe3	2.762(2)	2.737(1)
av Mo–S	2.322	2.327
Range	2.313(2)–2.329(2)	2.321(2)–2.332(2)
av Fe–S	2.282	2.276
Range	2.272(3)–2.299(3)	2.262(2)–2.280(2)
av Fe–X	2.200	2.540
Range	2.196(3)–2.205(3)	2.534(1)–2.547(1)
S–Mo–S	103.09	103.47
Range	102.81(8)–103.28(8)	103.37(6)–103.59(6)
Fe–Mo–Fe	59.84	59.67
Range	59.32(4)–60.22(4)	59.07(3)–59.99(3)
Mo–Fe–Fe	60.08	60.16
Range	59.62(4)–60.47(4)	59.88(3)–60.47(3)
Fe–Fe–Fe	60.00	60.00
Range	59.09(5)–60.57(5)	59.01(4)–60.52(3)
Mo–S–Fe	73.67	72.89
Range	73.48(8)–73.86(7)	72.76(5)–73.00(5)
Fe–S–Fe	74.14	73.49
Range	72.94(7)–74.88(8)	72.50(6)–74.14(6)
Mo–Fe–X	143.03	143.71
Range	140.21(9)–144.76(9)	141.15(4)–145.36(4)
S–Fe–X	114.1	113.73
Range	110.9(1)–118.8(1)	112.00(6)–117.54(6)

3.2. Reactions of $[Cp^*MoFe_3S_4X_3]^-$ (X = Cl, I) with P^tBu_3 and ArNC

The majority of transition metal sulfide clusters carry negative charges and are soluble only in polar solvents, where partial dissociation of anionic ligands often hampers isolation of meta-stable cluster structures. In this respect, synthesis of neutral $MoFe_3S_4$ clusters is attractive, because they may be dissolved in non-polar solvents, and assemblage of metal sulfide clusters in non-polar solvents would expand the scope of cluster synthesis. In fact, we were successful in isolating a $[Fe_8S_7]$ cluster complex relevant to the nitrogenase P-cluster, from a self-assembly reaction of Fe(II) bis-amide, tetramethylthiourea (tmtu), 2,4,6-triisopropylbenzenethiol (HStip), and elemental sulfur (S_8) in toluene [16]. We thus investigated the reactions of **4** and **5** with isocyanides and phosphines, aiming at isolation of neutral $MoFe_3S_4$ clusters.

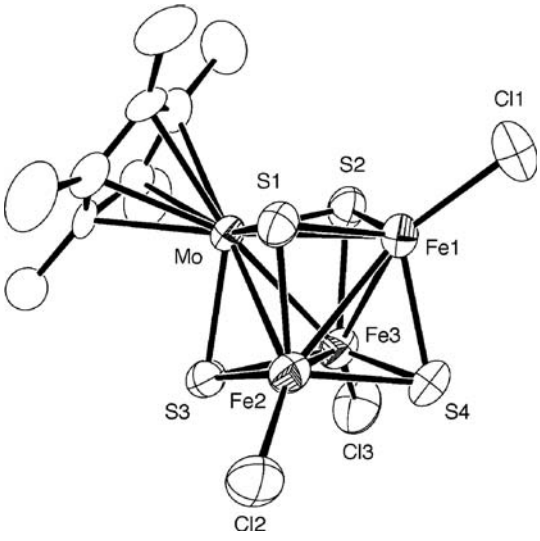

Fig. 1. Structure of the cluster anion of **4**, showing 50% probability ellipsoids and the atom-labeling scheme.

When **5** was treated with a slight excess of P^tBu_3 in CH_3CN, one of the iodide ligands came off as PPh_4I, and the void was occupied by phosphine, giving rise to a neutral cluster $Cp^*MoFe_3S_4I_2(P^tBu_3)$ (**6**) as black crystals in 71% yield. This neutral cluster is highly soluble in THF. In this reaction, no redox process is involved, and the formal electronic configuration of $[MoFe_3S_4]^{3+}$ remains intact. On the other hand, analogous ligand substitution of **4** did not occur, and attempts to prepare the chloride analogue $Cp^*MoFe_3S_4Cl_2(P^tBu_3)$ have failed. The different reactivity between **4** and **5** toward P^tBu_3arises probably from the weaker Fe–I bond of **5** relative to the Fe–Cl bond of **4**. Interestingly, the reactions of cubane clusters $[Fe_4S_4X_4]^{2-}$ (X = Cl, Br, I) and $[(Cl_4cat)(CH_3CN)MoFe_3S_4Cl_3]^{2-}$ with bulky tertiary phosphine were reported to occur in the presence of $NaBPh_4$, yielding the neutral clusters $Fe_4S_4X(P^tBu_3)_3$ [17] and $(Cl_4cat)(CH_3CN)MoFe_3S_4(PR_3)_3$ (R = ^{t}Bu, ^{i}Pr) [8b], respectively. During these reactions, the cubane core was reduced from $[Fe_4S_4]^{2+}$ or $[MoFe_3S_4]^{3+}$ to $[Fe_4S_4]^{+}$ or $[MoFe_3S_4]^{2+}$, where phosphine appeared to act as a reducing agent

$(PPh_4)[Cp^*MoFe_3S_4I_3]$

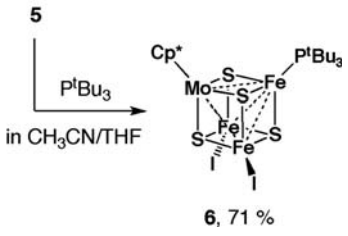

(4)

The X-ray-derived molecular structure of **6** is presented in Fig. 2, and selected bond distances and angles are listed in Table 4. The geometrical parameters of **6** are nearly identical to those of **5**, and the substitution of one iodide ligand by P^tBu_3 hardly changed the $[MoFe_3S_4]^{3+}$ core geometry of **5**. This is reasonable, because the transformation from **5** to **6** does not involve a redox process. The Fe1–P distance of 2.4306(8) Å is slightly shorter than those found for $(Cl_4cat)(CH_3CN)MoFe_3S_4(P^tBu_3)_3$ (av. 2.453 Å) [8b], $Fe_4S_4(P^tBu_3)_3Cl$ (av. 2.458(7) Å) [17], and $[Fe_4S_4(P^tBu_3)_4](BPh_4)$ (av. 2.458(9) Å) [6f]. The cyclic voltammogram of **6** was measured in THF, which shows one irreversible oxidation at 0.15 V vs. SCE and two quasi-reversible reduction at −0.48 V and −0.80 V. These values are compared with the redox potentials of **2**, **4**,

and **5** in Table 2. Evidently, the neutral cluster **6** is more easily reduced than anionic **5**, probably due to the difference in the overall charge.

The iron sulfide clusters $[Fe_4S_4X_4]^{2-}$ (X = Cl, Br) were reported to react with RNC (R = ^{t}Bu, CH_3), resulting in the corresponding neutral clusters $Fe_4S_4X_2(RNC)_6$ [18]. In these reactions, the $[Fe_4S_4]^{2+}$ core is not reduced. Our attempts to react **4** and **5** with ^{t}BuNC and ArNC (ArNC = 2,6-diisopropylphenylisocyanide), however, did not lead to isolable products. On the other hand, the reduction of $[Fe_4S_4I_4]^{2-}$ was recently attained by cobaltocene in the presence of arylisocyanide, and yet another neutral cluster $Fe_4S_4I(2,6\text{-}Me_2C_6H_3NC)_9$ was obtained [6h]. The electrochemical data shown in Table 2 indicate that **4** and **5** could also be reduced by cobaltocene (−0.91 V vs. SCE) [19]. Therefore, we examined the reactions of **4** and **5** with cobaltocene in the presence of 1 equiv of ArNC. In the case of **4**, the reduction reaction occurred in a complicate manner, involving a metal-displacement of the $MoFe_3S_4$ core, from which we were able to isolate only an $[Fe_4S_4]^+$ cluster $Fe_4S_4Cl(ArNC)_9$ (**7**) as black crystals. The cluster **7** was characterized based on IR and elemental analysis, where **7** was crystallized with THF as a crystal solvent. In contrast, the reduction of **5** by cobaltocene proceeded as was expected, and an cationic cubane cluster $[Cp^*MoFe_3S_4(ArNC)_7]I$ (**8**) was obtained as dark brown crystals in a good yield. During the reaction, the cluster core $[MoFe_3S_4]^{3+}$ was reduced to $[MoFe_3S_4]^{2+}$. The IR spectrum of **8** shows a N≡C stretching band at 2080 cm^{-1}, while the N≡C bands of **7** appear at 2060 and 2100 cm^{-1}. The cyclic voltammogram of **8** was recorded in THF, and the data are added to Table 2. A quasi-reversible redox couple in the region of reduction was observed at the potential ($E_{1/2}$) more negative than those of **4**–**6**. This trend is understandable because the $[MoFe_3S_4]^{2+}$ core of **8** is more electron rich, and thus more difficult to be reduced, than the $[MoFe_3S_4]^{3+}$ core of **4**–**6**. In this regard, it is interesting that the corresponding $E_{1/2}$ values of **2** are more negative than that of **8**

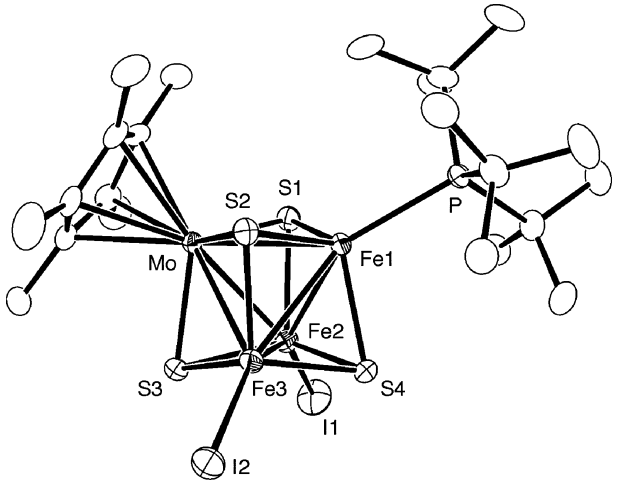

Fig. 2. Structure of **6**, showing 50% probability ellipsoids and the atom-labeling scheme.

Table 4
Selected bond distances (Å) and angles (°) for $Cp^*MoFeS_4I_2(P^tBu_3)$ (**6**)

Mo–Fe1	2.7256(4)	Fe1–P	2.4306(8)
Mo–Fe2	2.7372(5)	Fe2–I1	2.5356(5)
Mo–Fe3	2.7454(4)	Fe3–I2	2.5260(4)
Fe1–Fe2	2.6839(6)	av Mo–S	2.3232
Fe1–Fe3	2.7225(6)	Range	2.3152(7)–2.3301(7)
Fe2–Fe3	2.7497(6)	av Fe–S	2.2690
		Range	2.2311(8)–2.2870(8)
av S–Mo–S	103.25	av Fe–Fe–I	146.33
Range	102.94(3)–103.74(3)	Range	142.69(2)–149.23(2)
av Fe–Mo–Fe	59.58	av S–Fe–I	114.07
Range	58.85(1)–60.20(1)	Range	110.35(2)–119.52(3)
av Mo–Fe–Fe	60.56		
Range	60.36(1)–60.79(1)	S1–Fe1–P	111.01(3)
av Fe–Fe–Fe	60.00	S2–Fe1–P	120.03(3)
Range	58.74(1)–61.14(1)	S4–Fe1–P	108.98(3)
av Mo–S–Fe	73.09	Mo–Fe2–I1	144.33(2)
Range	72.79(2)–73.41(2)	Mo–Fe3–I2	138.79(2)
av Fe–S–Fe	73.67	Mo–Fe1–P	149.67(2)
Range	72.08(2)–75.06(3)	Fe2–Fe1–P	136.63(2)
Fe3–Fe1–P	145.30(2)		

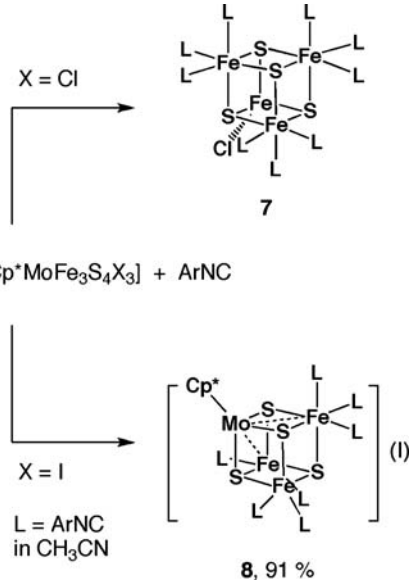

(5)

According to the X-ray analysis, an asymmetric unit of crystals of **8** consists of one cationic cubane cluster of $[Cp^*MoFe_3S_4(ArNC)_7]$, one discrete iodide, and two toluene molecules. The structure of the cluster cation is presented in Fig. 3, and selected bond distances and angles are listed in Table 5. To the cuboidal $MoFe_3S_4$ frame, one Cp^* and seven isocyanide ligands are bound. Given seven isocyanides, coordination geometries of the three irons are not chemically equivalent. There are one octahedral Fe atom carrying three isocyanide ligands, and two trigonal-bipyramidal Fe atoms with two isocyanide. As a consequence, the $MoFe_3S_4$ core structure of **8** departs markedly from those of **4**–**6**. The most notable deformation comes from elongation of the meal–metal and iron–sulfur

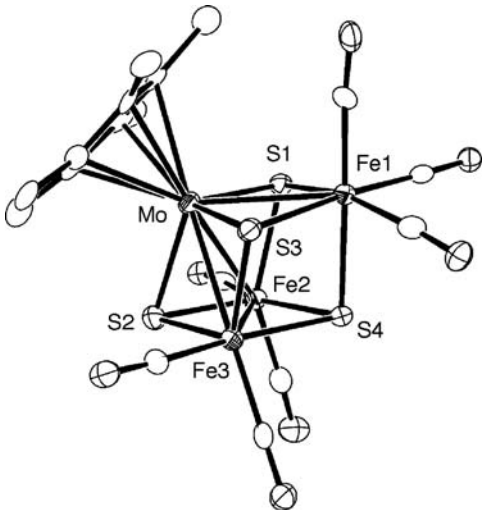

Fig. 3. Structure of the cluster cation of **8**, showing 50% probability ellipsoids and the atom-labeling scheme. The aryl groups of isocyanide are omitted for clarity.

distances associated with the octahedral Fe. Both the Mo–Fe(octahedral) distance of 2.915(2) Å and Fe(octahedral)–Fe(trigonal-bipyramidal) distances of 3.367(2) Å and 3.352(2) Å are substantially longer than the corresponding metal–metal distances of **4**–**6**, while the other metal–metal distances of **8** are comparable to **4**–**6**. It appears that the octahedral Fe is electronically saturated and does not form strong metal–metal bonds. Likewise, the Fe(octahedral)–S bond lengths (av. 2.322 Å) are longer than those of **4**–**6**, and than Fe(trigonal-bipyramidal)–S bonds (av. 2.233 Å). A similar distortion of the $MoFe_3S_4$ core geometry was observed for $[MoFe_3S_4(S_2CNEt_2)_5]^-$ and $MoFe_3S_4(S_2CNR_2)_5$ (R = Et, Bu, C_5H_{10}) [20]. The other intriguing geometrical features of **8** are the planar arrangement of Fe2, Fe3, S2, and S4, and the relatively short Fe2–S2 and F3–S2 bonds concomitant with the long Mo–S2 bond.

Noteworthy here is difference in the coordination geometries at Fe between **8** and **7** (or $Fe_4S_4I(2,6\text{-}Me_2C_6H_3NC)_9$) [6h]. For the latter two Fe_4S_4 clusters, aside from the tetrahedral Fe atom which binds chloride (or iodide), each of the remaining three Fe atoms carries three isocyanides, whereas for **8** two Fe atoms each binds only two isocyanides. This may be attributed to the steric bulk of Cp^*, or to the electronic property characteristic of the Cp^*Mo moiety in the $[MoFe_3S_4]$ cluster.

Table 5
Selected bond distances (Å) and angles (°) for $[Cp^*MoFeS_4(ArNC)_7]I$ (**8**)

Mo–Fe1	2.915(2)	Fe1–S1	2.314(3)
Mo–Fe2	2.746(2)	Fe1–S3	2.326(3)
Mo–Fe3	2.752(2)	Fe1–S4	2.325(3)
Fe1–Fe2	3.367(2)	Fe2–S1	2.267(3)
Fe1–Fe3	3.352(2)	Fe2–S2	2.173(3)
Fe2–Fe3	2.665(2)	Fe2–S4	2.248(3)
Mo–S1	2.291(3)	Fe3–S2	2.183(3)
Mo–S2	2.348(3)	Fe3–S3	2.245(3)
Mo–S3	2.297(3)	Fe3–S4	2.284(3)
Fe1–C11	1.84(1)	N1–C11	1.16(1)
Fe1–C24	1.85(1)	N2–C24	1.18(1)
Fe1–C37	1.85(1)	N3–C37	1.16(1)
Fe2–C50	1.81(1)	N4–C50	1.18(1)
Fe2–C63	1.84(1)	N5–C63	1.18(1)
Fe3–C77	1.84(1)	N6–C77	1.16(1)
Fe3–C89	1.84(1)	N7–C89	1.15(1)
Fe1–Mo–Fe2	72.92(4)	Mo–S1–Fe1	78.54(8)
Fe1–Mo–Fe3	72.46(4)	Mo–S1–Fe2	74.10(8)
Fe2–Mo–Fe3	58.00(4)	Mo–S2–Fe2	74.68(8)
Mo–Fe1–Fe2	51.22(4)	Mo–S2–Fe3	74.70(9)
Mo–Fe1–Fe3	51.52(3)	Mo–S3–Fe2	78.17(8)
Mo–Fe2–Fe1	55.86(4)	Mo–S3–Fe3	74.59(8)
Mo–Fe2–Fe3	61.12(4)	Fe1–S1–Fe2	94.61(9)
Mo–Fe3–Fe1	56.02(4)	Fe2–S2–Fe3	75.45(9)
Mo–Fe3–Fe2	60.88(4)	Fe1–S3–Fe3	94.3(1)
		Fe1–S4–Fe2	94.8(1)
		Fe1–S4–Fe3	93.3(1)
		Fe2–S4–Fe3	72.04(9)
Fe1–C11–N1	171.9(9)	C11–N1–C12	175(1)
Fe1–C24–N2	172.8(9)	C24–N2–C25	166.2(9)
Fe1–C37–N3	176.7(9)	C37–N3–C38	169(1)
Fe2–C50–N4	175.7(8)	C50–N4–C51	170(1)
Fe2–C63–N5	175.5(9)	C63–N5–C64	174(1)
Fe3–C76–N6	174.3(9)	C76–N6–C77	173(1)
Fe3–C89–N7	177.3(9)	C89–N7–C90	166(1)

4. Supplementary material

Crystallographic data for the structures reported in this paper have been deposited with the Cambridge Crystallographic Data Centre, CCDC No. 609450 for compound **4**, CCDC No. 609451 for compound **5**, CCDC No. 609452 for compound **6**, and CCDC No. 609453 for compound **8**. Copies of this information may be obtained free of charge from the Director, CCDC, 12 Union Road, Cambridge CB2 1EZ, UK (fax: +44 1223 336033; e-mail: deposit@ccdc.cam.ac.uk or www: http://www.ccdc.cam.ac.uk).

Acknowledgements

This research was financially supported by Grant-in-Aids for Scientific Research on Priority Area (Nos. 14078101 and 14078211 "Reaction Control of Dynamic Complexes") from the Ministry of Education, Culture, Sports, Science, and Technology, Japan.

References

[1] (a) H. Beinert, R.H. Holm, E. Münck, Science 277 (1997) 653;
(b) M.D. Curtis, S.H. Druker, J. Am. Chem. Soc. 119 (1997) 1027.
[2] E.I. Stiefel, K. Matsumoto, Transition Metal Sulfur Chemistry, Biological and Industrial Significance, American Chemical Society, Washington, DC, 1996.
[3] (a) B. Schmid, M.W. Ribbe, O. Einsle, M. Yoshida, L.M. Thomas, D.R. Dean, D.C. Rees, B.K. Burgess, Science 296 (2002) 352;
(b) M.-H. Suh, L. Pulakat, N.J. Gavini, Biol. Chem. 278 (2003) 5353;
(c) O. Einsle, F.A. Tezcan, L.A. Andrade, B. Schmidt, M. Yoshida, J.B. Howard, D.C. Rees, Science 297 (2002) 1969.
[4] (a) A. Müller, E. Diemann, R. Jostes, H. Bögge, Angew. Chem., Int. Ed. Engl. 20 (1981) 934;
(b) D. Coucouvanis, Acc. Chem. Res. 14 (1981) 201;
(c) R.H. Holm, Adv. Inorg. Chem. 38 (1992) 1;

(d) N.C. Payne, N. Okura, S. Otsuka, J. Am. Chem. Soc. 105 (1983) 245;
(e) S.-W. Lu, N. Okura, T. Yoshida, S. Otsuka, K. Hirotsu, T. Higuchi, J. Am. Chem. Soc. 105 (1983) 7470;
(f) Y. Arikawa, H. Kawaguchi, K. Kasiwabara, K. Tatsumi, Inorg. Chem. 38 (1999) 4549.

[5] (a) S. Kabashima, S. Kuwata, M. Hidai, J. Am. Chem. Soc. 121 (1999) 7837;
(b) T. Ikeda, S. Kuwata, Y. Mizobe, M. Hidai, Inorg. Chem. 37 (1998) 5793;
(c) M. Hidai, S. Kuwata, Y. Mizobe, Acc. Chem. Res. 33 (2000) 46;
(d) M.A. Mansour, M.D. Curtis, J.W. Kampf, Organometallics 16 (1997) 275;
(e) P. Li, M.D. Curtis, Inorg. Chem. 29 (1990) 1242;
(f) P. Braunstein, A. Tiripicchio, M. Tiripicchio-Camellini, E. Sappa, Inorg. Chem. 20 (1981) 3586;
(g) B.A. Cowans, R.C. Haltiwanger, M. Rakowski DuBois, Organometallics 6 (1987) 995;
(h) T. Shibahara, Adv. Inrog. Chem. 37 (1991) 143;
(i) R. Hernández-Molina, A.G. Sykes, J. Chem Soc., Dalton Trans. (1997) 3137.

[6] (a) D. Coucouvanis, Acc. Chem. Res. 24 (1991) 1;
(b) D. Coucouvanis, P.R. Challen, S.-M. Koo, M.W. Davis, W. Butler, W.R. Dunham, Inorg. Chem. 28 (1989) 4187;
(c) P.R. Challen, S.-M. Koo, W.R. Dunham, D. Coucouvanis, J. Am. Chem. Soc. 112 (1990) 2455;
(d) P.R. Challen, S.-M. Koo, C.G. Kim, W.R. Dunham, D. Coucouvanis, J. Am. Chem. Soc. 112 (1990) 8606;
(e) L. Cai, B.M. Segal, J.R. Long, M.J. Scott, R.H. Holm, J. Am. Chem. Soc. 117 (1995) 8863;
(f) C. Goh, B.M. Segal, J. Huang, J.R. Long, R.H. Holm, J. Am. Chem. Soc. 118 (1996) 11844;
(g) J. Huang, S. Mukerjee, B.M. Segal, H. Akashi, J. Zhou, R.H. Holm, J. Am. Chem. Soc. 119 (1997) 8662;
(h) J.-P. Lang, K. Tatsumi, H. Kawaguchi, J.-M. Lu, P. Ge, W. Ji, S. Shin, Inorg. Chem. 35 (1996) 7924;
(i) M. Harmjanz, W. Saak, D. Haase, S. Pohl, Chem. Commun. (1997) 952;
(j) J.-P. Lang, K. Tatsumi, Inorg. Chem. 37 (1998) 6308;
(k) H. Yu, Q.-F. Xu, Z.-R. Sun, S.-J. Ji, J.-X. Chen, Q. Liu, J.-P. Lang, K. Tatsumi, Chem. Commun. (2001) 2614.

[7] (a) H. Kawaguchi, K. Tatsumi, J. Am. Chem. Soc. 117 (1995) 3885;
(b) H. Kawaguchi, K. Yamada, J.-P. Lang, K. Tatsumi, J. Am. Chem. Soc. 119 (1997) 10346;
(c) J.-P. Lang, H. Kawaguchi, S. Ohnishi, K. Tatsumi, J. Chem. Soc., Chem. Commun. (1997) 405;
(d) K. Tatsumi, J.-P. Lang, S. Ohnishi, T. Nagasawa, H. Kawaguchi, J. Inorg. Biochemi. 67 (1997) 269;
(e) J.-P. Lang, H. Kawaguchi, K. Tatsumi, Inorg. Chem. 36 (1997) 6447;
(f) J.-P. Lang, K. Tatsumi, Inorg. Chem. 37 (1998) 160;
(g) J.-P. Lang, H. Kawaguchi, K. Tatsumi, J. Organomet. Chem. 569 (1998) 109;
(h) J.-P. Lang, K. Tatsumi, Inorg. Chem. 38 (1999) 1364;
(i) J.-P. Lang, K. Tatsumi, J. Organomet. Chem. 579 (1999) 332;
(j) J.-P. Lang, H. Kawaguchi, K. Tatsumi, J. Chem. Soc., Chem. Commun. (1999) 2315;
(k) J.-P. Lang, Q.-F. Xu, W. Ji, H.I. Elim, K. Tatsumi, Eur. J. Inorg. Chem. (2004) 86.

[8] (a) K.D. Demadis, C.F. Campana, D. Coucouvanis, J. Am. Chem. Soc. 117 (1995) 7832;
(b) F. Osterloh, B.M. Segal, C. Achim, R.H. Holm, Inorg. Chem. 39 (2000) 980.

[9] H. Kawaguchi, K. Yamada, S. Ohnishi, K. Tatsumi, J. Am. Chem. Soc. 119 (1997) 10871.

[10] P.C.J. Kamer, R.J.M. Nolte, W. Drenth, J. Am. Chem. Soc. 110 (1988) 6818.

[11] R.B. King, Organometall. Synth. 1 (1965) 70.

[12] (a) K.S. Hagen, A.D. Watson, R.H. Holm, J. Am. Chem. Soc. 105 (1983) 3905;
(b) G. Christou, C.D. Garner, J. Chem. Soc., Dalton. Trans. (1978) 1093.

[13] (a) D. Coucouvanis, S.-J. Chen, B.S. Mandimutsira, C.G. Kim, Inorg. Chem. 33 (1994) 4429;
(b) K.D. Demadis, D. Coucouvanis, Inorg. Chem. 34 (1995) 3658.

[14] (a) G.B. Wong, M.A. Bobrik, R.H. Holm, Inorg. Chem. 17 (1978) 578;
(b) R.E. Palermo, R.H. Holm, J. Am. Chem. oc. 105 (1983) 4310;
(c) R.W. Johnson, R.H. Holm, J. Am. Chem. Soc. 100 (1978) 5338;
(d) D. Coucouvanis, S. Al-Abmad, A. Salifoglou, V. Papaefthymiou, A. Kostikas, A. Simpoulos, J. Am. Chem. Soc. 114 (1992) 2472.

[15] K.D. Demadis, D. Coucouvanis, Inorg. Chem. 34 (1995) 436.

[16] Y. Ohki, Y. Sunada, M. Honda, M. Katada, K. Tatsumi, J. Am. Chem. Soc. 125 (2003) 4052.

[17] M.A. Tyson, K.D. Demadis, D. Coucouvanis, Inorg. Chem. 34 (1995) 4519.

[18] (a) J.A. Weigel, K.K.P. Srivastava, E.P. Day, E. Münck, R.H. Holm, J. Am. Chem. Soc. 112 (1990) 8015;
(b) C. Goh, J.A. Weigel, R.H. Holm, Inorg. Chem. 33 (1994) 4861.

[19] D. O'Hare, J.C. Green, T. Marder, S. Collins, G. Stringer, A.K. Kakkar, N. Kaltsoyannis, A. Kuhn, R. Lewis, C. Mehnert, P. Scott, M. Kurmoo, S. Pugh, Organometallics 11 (1992) 58.

[20] S. Harris, Polyhedron 8 (1989) 2843.